A trapped magnetic field of 3 T in homogeneous, bulk MgB$_2$ superconductors fabricated by a modified precursor infiltration and growth process

A trapped magnetic field of 3 T in homogeneous, bulk MgB$_2$ superconductors fabricated by a modified precursor infiltration and growth process

A G Bhagurkar[1], A Yamamoto[2], L Anguilano[3], A R Dennis[4], J H Durrell[4], N Hari Babu[1] and D A Cardwell[4]

[1] Brunel Centre for Advanced Solidification Technology, Brunel University London, Uxbridge, UB8 3PH, UK
[2] Department of Applied physics, Tokyo University of Agriculture and Technology, 2-24-16 Nakacho, Koganei, Tokyo 184-8588, Japan
[3] Experimental Techniques Centre, Brunel University London, Uxbridge, UB8 3PH, UK
[4] Bulk Superconductivity Group, Department of Engineering, University of Cambridge, Trumpington Street, CB2 1PZ, UK

E-mail: ashutosh.bhagurkar@brunel.ac.uk

Abstract

The wetting of boron with liquid magnesium is a critical factor in the synthesis of MgB$_2$ bulk superconductors by the infiltration and growth (IG) process. Poor wetting characteristics can therefore result potentially in non-uniform infiltration, formation of defects in the final sample structure and poor structural homogeneity throughout the bulk material. Here we report the fabrication of near-net-shaped MgB$_2$ bulk superconductors by a modified precursor infiltration and growth (MPIG) technique. A homogeneous bulk microstructure has subsequently been achieved via the uniform infiltration of Mg liquid by enriching pre-reacted MgB$_2$ powder within the green precursor pellet as a wetting enhancer, leading to relatively little variation in superconducting properties across the entire bulk sample. Almost identical values of trapped magnetic field of 2.12 T have been measured at 5 K at both the top and bottom surfaces of a sample fabricated by the MPIG process, confirming the uniformity of the bulk microstructure. A maximum trapped field of 3 T has been measured at 5 K at the centre of a stack of two bulk MgB$_2$ samples fabricated using this technique. A steady rise in trapped field was observed for this material with decreasing temperature down to 5 K without the occurrence of flux avalanches and with a relatively low field decay rate (1.5%/d). These properties are attributed to the presence of a fine distribution of residual Mg within the bulk microstructure generated by the MPIG processing technique.

Keywords: MgB2, infiltration and growth, trapped field

(Some figures may appear in colour only in the online journal)

Introduction

The ability of a type II bulk superconductor to trap magnetic field is a direct indication of the presence of strong flux pinning, and hence high critical current density, J_c, within the sample microstructure. In general, the magnitude of the field trapped by a bulk superconductor is determined by the product of the sample radius, r, and J_c, assuming that the current flows homogeneously throughout the volume of the sample. As a result, superconducting 'permanent magnets' have the
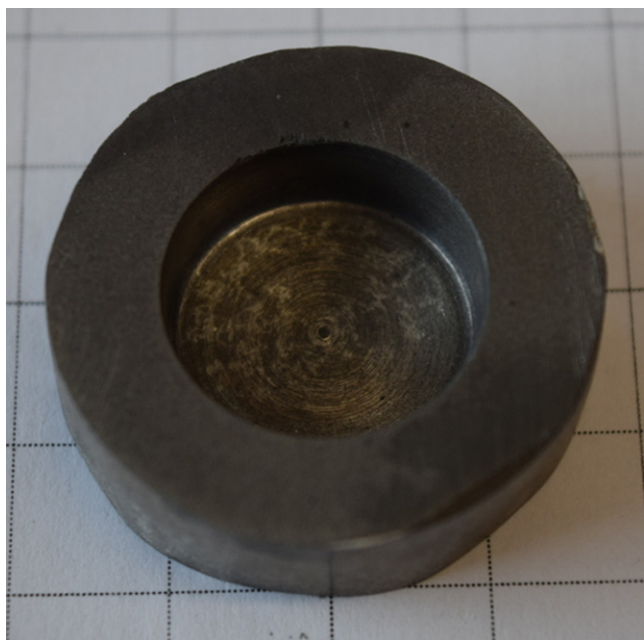
Figure 1. A MgB_2 cavity structure of depth 6 mm and diameter 18 mm.

potential to generate magnetic fields that are significantly higher than conventional Nd-Fe-B magnets, which are limited generally to less than 2 T. MgB_2 superconductors, in particular, have already been used to generate trapped fields of greater than 5 T [1, 2]. Furthermore, the relatively high T_c (39 K), low raw material cost, lower density, relative ease of fabrication and ability of grain boundaries to support supercurrent make this material an exciting choice for practical applications. Techniques to fabricate bulk MgB_2 mainly include sintering (either *in situ* or *ex situ*) and those based on an infiltration process (such as reactive liquid infiltration (RLI) or infiltration and growth (IG)), both of which offer certain advantages. *In situ* sintering, for example, can be used generally to produce a well-connected MgB_2 phase with relative ease [3], whereas the infiltration method is useful for the fabrication of near net shaped, dense MgB_2 bulk materials, as reported by Giunchi *et al* [4, 5]. This is illustrated by the closed end cavity fabricated using an infiltration technique discussed later, as shown in figure 1, which required only minimum post-processing machining to obtain a smooth inner cavity surface.

A significant increase in trapped field has been reported recently for sintered MgB_2 bulk samples. Notably, Fuchs *et al* and Yamamoto *et al* reported high trapped fields of 5.4 T (12 K) and 3.72 T (5 K) respectively, in nano-crystalline MgB_2 samples [1, 6]. In addition, Yamamoto *et al* reported a trapped field of 4 T at 10 K in an *in situ* sintered MgB_2 sample and Naito *et al* obtained 4.6 T in a Ti-doped MgB_2 bulk at 14 K [7, 8]. Finally, Durrell *et al* reported 3 T at 17.5 K in a sintered, hot-uniaxially pressed MgB_2 bulk sample fabricated by an *ex situ* technique [9]. These recent data represent a significant improvement over the previous reports of the field trapping ability of MgB_2 of Viznichenko *et al* Murlidhar *et al*

Naito *et al* Perini *et al* and Giunchi *et al* [10–14]. However these levels of field have not yet been realized in samples fabricated by an infiltration technique [13–15], although samples processed by infiltration route are denser and the local critical current density in samples fabricated by the two methods is comparable [16–20].

Several existing reports [16, 21–23] and more recent studies by the current authors [19, 20] indicate that all infiltration processes generate a considerable amount of residual Mg, up to 20%, in the fully processed sample microstructure, due primarily to 25% volume shrinkage in MgB_2 during the phase formation process. This makes way for the surrounding liquid Mg during the primary phase formation process, assuming that MgB_2 nucleates everywhere simultaneously in the precursor and that the sample does not shrink overall. Giunchi *et al* observed the presence of residual Mg both in the form of discrete, fine inclusions between large MgB_2 particles and as thread-like structures ($\sim$20 μm long) in individual MgB_2 particles in RLI process [16]. This is consistent with our recent studies. In addition, we also observed a large number of continuous Mg channels extending from the surface of bulk MgB_2 sample to its centre, as illustrated in figure 2(a) [20]. Such samples generally exhibit very low trapped fields, despite their superior local superconducting properties, since concentric current loops that form in the superconductor are impeded by these non-superconducting Mg channels. It is apparent, therefore, that the presence of residual Mg, especially in the form of continuous channels, may have an adverse effect on the trapped field performance of MgB_2 bulk superconductors fabricated by an IG process.

In RLI processed samples, Naito *et al* suggested casing the precursor with a stainless steel to curb any expansion of sample in radial direction [23]. This approach ameliorated the problem of continuous unreacted Mg in the bulk. In this work, we aim to control the formation of residual Mg channels and to fabricate homogeneous MgB_2 bulk superconductors by incorporating MgB_2 powder as wetting enhancer in the IG process. The resulting spatial variation in superconducting properties of bulk samples fabricated by this technique and the trapped fields achieved are reported.

Initial studies on enriching B powder with MgB_2 prior to diffusion processing were reported by Iwayama *et al* [24]. This approach was effective to supress formation of voids and cracks that formed during the process, as a result of low and inhomogeneous filling density of boron powder [24–26].

Experiment

Sample preparation

Crystalline boron (98% pure, HC Starck, <38 μm) and MgB_2 powders (Pavezyum, <44 μm) were mixed thoroughly in a molar ratio of 90:10. The resulting powder mixture was pressed uniaxially into two cylindrical precursor pellets of
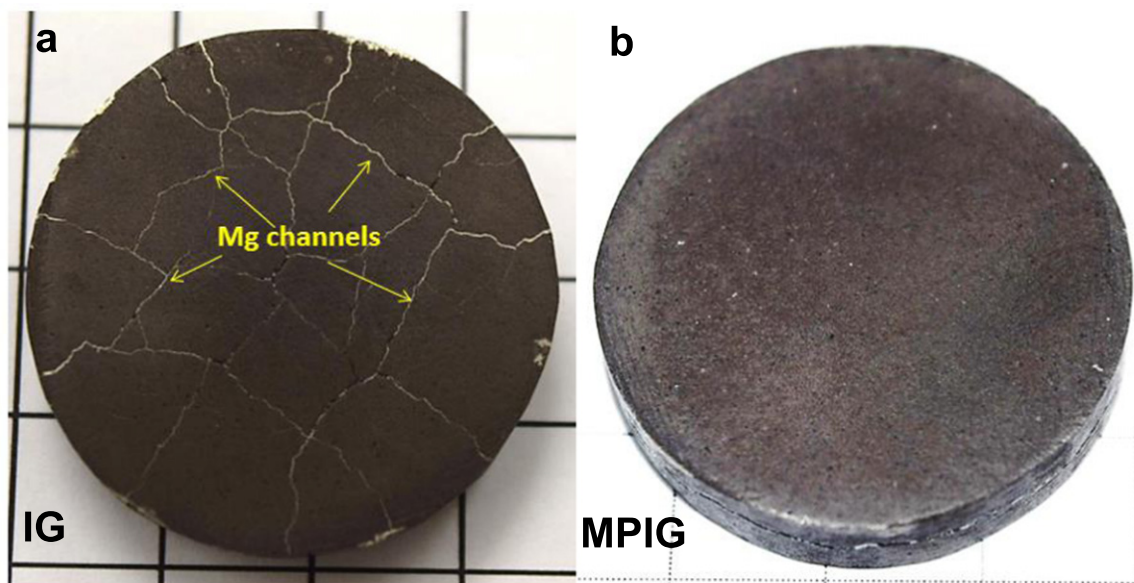
Figure 2. MgB$_2$ bulk samples fabricated by (a) infiltration and growth (IG) and (b) modified precursor infiltration and growth (MPIG) process. IG sample shows large population of Mg channels.

diameter 32 mm and thickness 6 mm under a load of 10 MPa. Magnesium was melted in a separate process and held at 700 °C in a graphite crucible. The precursor pellet, which was contained in a porous steel vessel, was transferred slowly to the crucible containing the liquid Mg. The use of the porous steel vessel ensured that that no part of precursor pellet came into contact with the walls of the crucible and that it did not float on the Mg melt, which could result potentially in a non-uniform infiltration process. Column height of Mg(l) was maintained at 10 cm above precursor to obtain a hydrostatic pressure of approximately 1.7% that of atmospheric pressure, which was found to be necessary to achieve a uniform infiltration process. The entire assembly was then subjected to the thermal profile reported in reference [20] and held at a reaction temperature of 850 °C for 4 h. A controlled, continuous flow of gas of a mixture of N$_2$ + SF$_6$ of volume ratio 95:5 was maintained over the sample during processing to minimize oxidation of Mg. SF$_6$ gas is known to react with Mg(l) to form MgF$_2$, which fills the pores in otherwise porous MgO film on the melt surface. This forms a continuous impervious MgO/MgF$_2$ layer on melt surface which protects underlying Mg from oxidation [27]. After the end of thermal cycle (at 700 °C), the steel vessel containing reacted product was taken out from the melt. The excess Mg surrounding the sample after processing was removed by grinding to recover the bulk specimen ($\rho \approx 2.45$ g cm^{-3}). The sample was then characterized using various physical property and compositional measurement techniques. The method of fabrication used in this study, based on a composite precursor containing 10 mol% MgB$_2$ powder, is referred to subsequently as the modified precursor infiltration and growth (MPIG) method, whereas IG is used to describe any method that uses a precursor pressed purely from boron powder.

Characterization

The microstructure of the sample fabricated by IG and MPIG process was studied by scanning electron microscopy. The magnetic moment of small specimens cut from the as-processed bulk was measured using a superconducting quantum interference device (SQUID) magnetometer. The critical current densities of these samples were calculated from measured magnetic moment hysteresis loops using the extended Bean model for a rectangular cross section in a perpendicular, applied magnetic field [28].

Physical property measurements

Two separate trapped field measurements were made, on an individual MPIG MgB$_2$ bulk sample, and on a two-sample stack, respectively, using the same measurement procedure in each case. Stacked arrangement was made primarily to minimize demagnetization effect, which is more severe in case of a single bulk. The measurements involved cooling down the sample or sample arrangement to 5 K under an external magnetic field of 5 T applied perpendicular to the top surface of the sample using a Gifford–McMahon cryocooler (CRTHE05-CSFM, Iwatani Gas). The external magnetic field was then reduced very slowly to zero at a rate of 1.8 T h^{-1} to minimize any loss of trapped flux from the sample(s), as shown in figure 3. The sample(s) was then heated slowly at 0.1 K min^{-1} and the trapped magnetic flux density was measured at temperatures up to 40 K by two cryogenic Hall sensors (HGCT-3020, Lake Shore). The Hall sensors were placed at the centre of the top and bottom surfaces of an individual bulk sample to enable the trapped field to be measured simultaneously in the first measurement. In the second measurement, one Hall probe was positioned at the centre of the top surface of the upper sample in a two sample
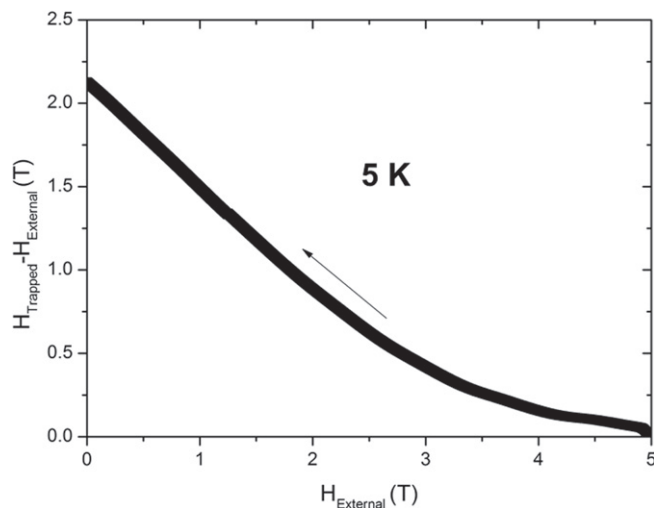
Figure 3. Difference between trapped magnetic flux density and external field as a function of external field for the MgB$_2$ bulk samples fabricated by MPIG.

stack, with the second probe used to measure the trapped field between the sample pair.

Results and discussion

Role of MgB$_2$ in the powder precursor

Figures 2(a) and (b) show photographs of the MgB$_2$ samples fabricated by IG and MPIG processes, respectively. The sample fabricated by IG exhibits a number of residual Mg channels that are not present in the sample fabricated by MPIG. As a result, the former underwent significant macroscopic expansion after processing whereas the latter retained its dimensions fairly closely. Furthermore, MPIG method has also enabled fabrication of homogeneous complex cavity structure (figure 1). The formation of continuous Mg channels in IG processing are believed to form due primarily to poor wetting between B(s) and Mg(l), which is further accentuated by volume shrinkage (by up to 25%) that occurs as a consequence of the Mg(l) + 2B(s) → MgB$_2$(s) reaction and hydrostatic pressure exerted by Mg(l) column on to the precursor during the infiltration process. The incorporation of MgB$_2$ powder enhanced the overall wettability of the precursor with Mg(l), which ensured uniform influx of Mg(l) into the pores. Moreover, the presence of MgB$_2$ powder in the precursor is observed to provide sufficient strength to withstand the compressive hydraulic stresses exerted by the Mg liquid. Also, presence of a wetting enhancer in the precursor pellet allows the precursor powder to be packed under higher uniaxial load, which directly benefits sintering and can potentially result high density of the processed sample.

Scanning electron microscopy

Figures 4(a) and (b) show SEM images of the polished surfaces of MgB$_2$ bulk samples fabricated MPIG process. Figure 4(b) shows the presence of two types of MgB$_2$

particles. Ones with a smooth surface and dark inner core and other that appears rough and bright. The particles with a dark-in-contrast boron rich, inner core comprise of B-rich intermediate (Mg$_2$B$_{25}$) phase [20]. These are almost certainly formed during the process, while the bright-in-contrast are pre-existing, unreacted MgB$_2$ particles. When a boron particle undergoes a reaction to transform into MgB$_2$ (i.e. 2 moles of B giving 1 mole of MgB$_2$), the original B particle almost doubles in volume, due to associated volume expansion (MgB$_{2(molar\ volume)}/2 \times$ B$_{(molar\ volume)}) \approx 2$). The growing MgB$_2$ particles then impinge upon each other and sinter simultaneously. This is evidenced by a large contact area between MgB$_2$ particles in the area shown by continuous contours in figures 4(a) and (b). Similar features were also observed elsewhere in the microstructure. However, such a large contact area was not observed between newly formed MgB$_2$ and pre-existing powder particles (dotted contours in figure 4(b)). This could be due to the fact that newly formed MgB$_2$ surface is free from impurities and therefore likely to sinter readily, whereas nano-scale impurities such as MgO and BO$_x$ are more likely to be present on the surface of pre-existing MgB$_2$ particles [29].

Spatial variation in MPIG samples

The uniformity of the superconducting properties throughout the volume of the MgB$_2$ cylinder, which is required to generate high trapped fields, was investigated by cutting nine, relatively large (4 mm × 3 mm × 2 mm) rectangular samples from various positions within the MPIG bulk. Figure 5(a) shows the normalized magnetization of these samples as a function of temperature, measured using a SQUID magnetometer. Typical magnetization data for IG-processed samples are also plotted for purposes of comparison. The measurements were made using a small, applied external magnetic field of 2 mT and normalized to the value at 30 K, with the position of the sample in the parent bulk indicated in the inset of figure 5(a). The IG processed sample exhibits a T_c of 37.50 K, whereas the samples cut from the MPIG bulk exhibit T_c's that vary between 37.25 and 37.40 K. Also, samples cut from rows 1 and 2 of the parent MPIG bulk exhibit very similar M–T curves with a sharp transition, whereas all the samples from row 3 (bottom surface) exhibit relatively broader transitions. XRD analysis (not shown here) on MPIG bulk shows presence of MgB$_2$, Mg and Mg$_2$B$_{25}$ phases with similar phase fraction on both top and bottom surfaces. Such M–T behaviour could be due possibly to the fact that slightly denser MgB$_2$, in comparison to boron, tends to settle preferentially towards the bottom of the precursor powder prior to palletization.

Figure 5(b) shows the dependence of external magnetic field on J_c for the MPIG specimens cut from the various sample locations. The geometrical location in the parent MPIG bulk sample appears to have little effect on J_c, which does not change appreciably across the volume of the bulk investigated. All the samples in MPIG bulk show J_c (5 K, 1 T) within the close range of ±10% of average J_c. This does not correlate directly to broad transitions observed
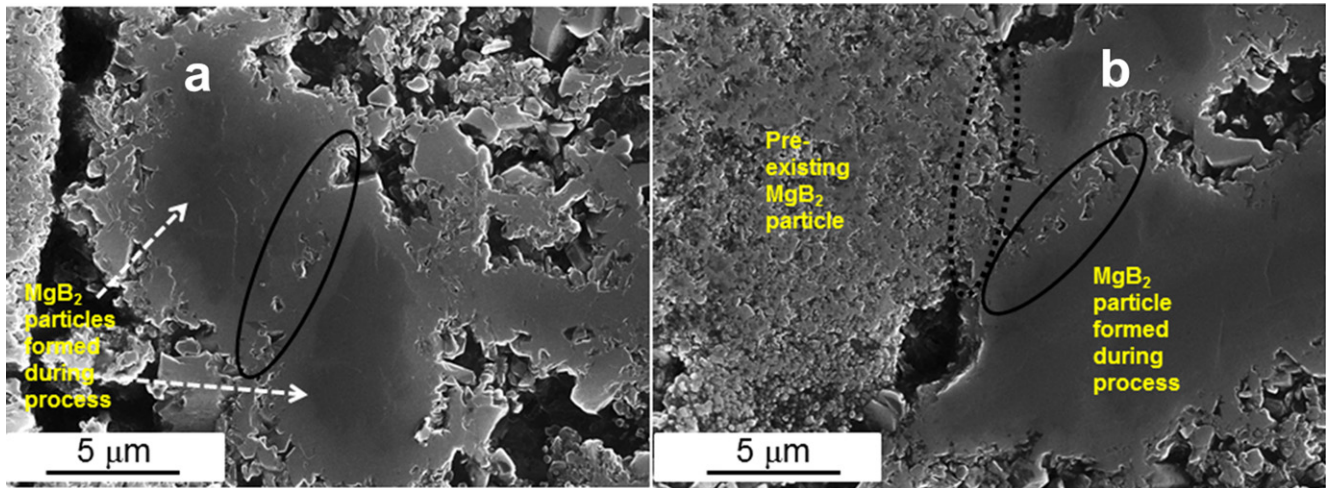
Figure 4. SEM micrographs showing different regions of the polished surface of MPIG processed bulk MgB_2 sample. Continuous contours (in (a) and (b)) indicate significant sintering between newly formed MgB_2 particles while dotted contours (b) show little inter-particle coupling between pre-existing MgB_2 particle with other particles.
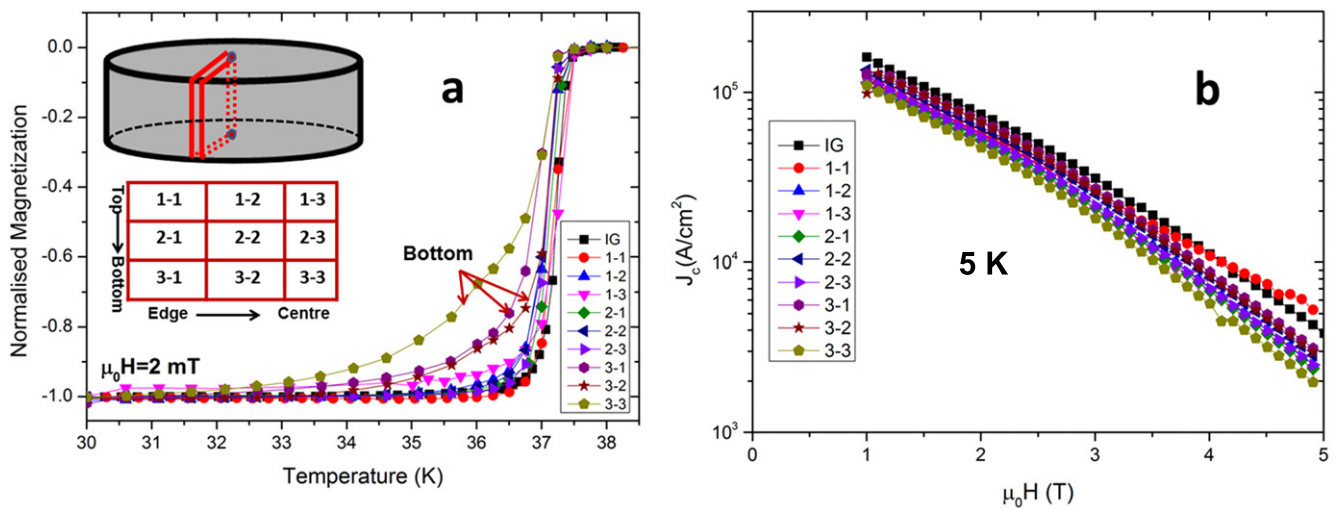

Figure 5. (a) Normalized M–T and (b) $J_c(B)$ (5 K) characteristics for nine samples cut from the locations in the parent bulk shown in the inset of figure 5(a) inset. The IG sample was cut from a location corresponding to 1–1, as shown in (a).

in some of the samples (figure 5(a)). This is because, at lower temperatures (5 K in this case), difference in ratio T/T_c is small enough in each sample to leave J_c $\left(\alpha\left[1-\left(\frac{T}{T_c}\right)^2\right]^{1.5}, \ \alpha \text{ being } J_c \text{ extrapolated to } 0 \text{ K}\right)$ almost unaltered from sample to sample [30]. MPIG and IG samples exhibit similar $J_c(B)$ dependence upto ∼3 T, after which MPIG samples show a strong $J_c(B)$ behaviour (except 1–1). Magneto optical studies on such bulks fabricated from pre-added MgB_2 powder by Polyanskii *et al* reveal that MgB_2 particles in microstructure have lower J_c than surrounding matrix. Origins of low J_c are reported to be weaker connectivity and lower H_{c2} that results in poor flux pinning strength [26].

These findings are consistent with SEM observations (figure 4) and J_c data reported here, which shows reduced J_c in MPIG bulk sample compared to IG sample. This suggests that the inter-grain electrical coupling between newly formed

MgB_2 particles (from boron during the processing) and pre-existing MgB_2 particles in the MPIG process is probably inferior compared to the coupling between two newly formed MgB_2 particles, These boundaries, therefore, probably form weak links at higher fields resulting in reduced J_c.

Trapped field measurements

The measured trapped field as a function of temperature for a single bulk and a stacked pair of MPIG processed bulk samples is shown in figures 6(a) and (b), respectively. A difference of less than 0.5% in the magnitude of trapped field recorded at the top and bottom surface of the single bulk confirms its homogeneity, given that any cracks, porosity or non-superconducting regions would impede the flow of supercurrent throughout the volume of the bulk. These measurements are consistent with narrow range of J_c (figure 5(b)) observed in the MPIG bulk. Although sample 3–3 (centre of
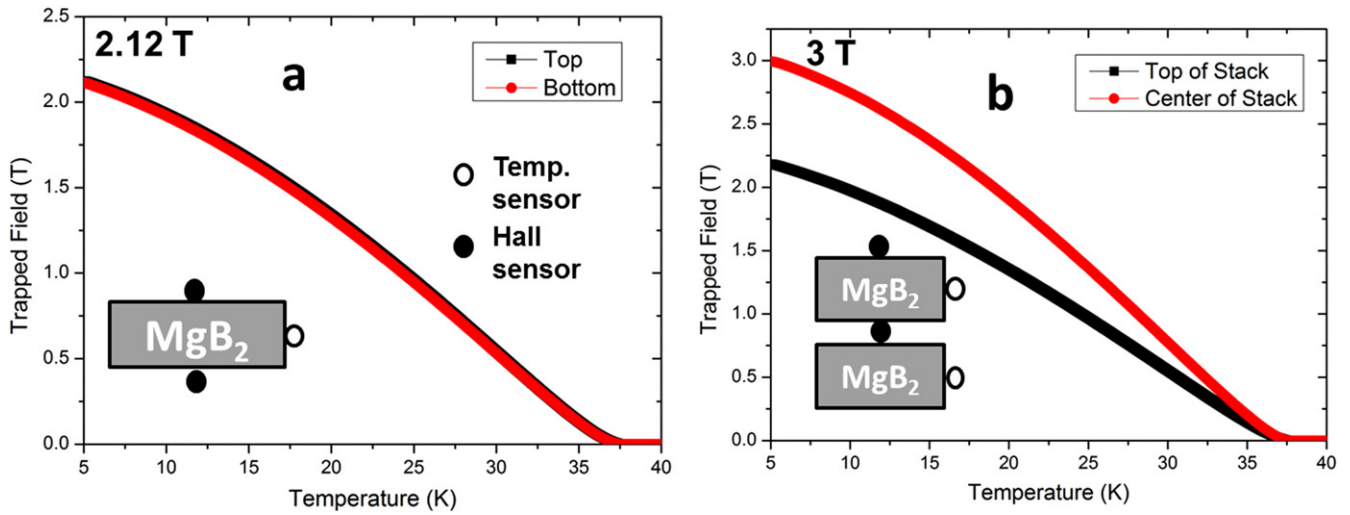
Figure 6. Trapped magnetic field for (a) a single bulk MgB$_2$ sample and (b) a two-sample stack geometry. The locations of the Hall and temperature sensors are shown in the insets.

bottom surface, figure 5) shows broad transition and low J_c amongst all samples, it is not likely to alter trapped field performance of MPIG bulk greatly. This is because the trapped field in the bulk is mainly governed by low field J_c in the outer regions of the bulk, as the current loop is largest. Recently, numerical simulations, based on a novel 2D axisymmetric **H**-formulation, have been performed for single a MPIG bulk sample using $J_c(B)$ data of single sub-specimen as an input for the model [31]. The model assumed, essentially, that the $J_c(B)$ characteristics of the small specimen extended over entire volume of the bulk sample. The results of the simulation reproduced the experimental results extremely well, confirming the homogeneity of the samples fabricated by the MPIG technique. Maximum trapped fields of 2.12 and 3 T were recorded for a single bulk and stacked pair of bulk samples, respectively. At 20 K, temperature that can easily achieved with cryogen free cost effective cryo-coolers, 1.35 and 2 T trapped field was recorded in a single bulk and centre of stack, respectively.

In comparison, for single bulk at 20 K, RLI processed sample trapped 1.1 T (55 mm dia, 15 mm thick) [13]. Yamamoto *et al* reported 1.9 T (30 mm dia, 10 mm thick) and Muralidhar *et al* reported 1.4 T (20 mm dia, 7 mm thick) in *in situ* sintered samples [11, 32]. High isostatically pressured samples showed 2 T (23 mm dia, 24 mm thick) [33]. Nanostructured bulk trapped 3.2 T (20 mm dia, 8 mm thick) and 2.2 T (30 mm dia, 10 mm thick) as reported by Fuchs *et al* and Sugino *et al* [1, 6]. Similarly Naito *et al* reported 2.8 T (40 mm dia, 20 mm thick) in Ti-doped bulk MgB$_2$ sample [8]. Whereas trapped field at the centre of 2 sample stack is reported 2.6 T in *ex situ* hot pressed, 2.9 T in *in situ* sintered and 3.6 T in Ti-doped MgB$_2$ bulk samples [7–9].

The Biot–Savart law suggests that trapped field is directly proportional to J_c and a dimensionless geometrical factor K, which depends on the radius of bulk sample;

$$B_T = \mu_0 \cdot J_c \cdot r \cdot k, \tag{1}$$

$$k = \frac{t}{2r} \ln\left(\frac{r}{t} + \sqrt{1 + \left(\frac{r}{t}\right)^2} \right), \tag{2}$$

where t and r are the thickness and radius of the sample, respectively [34]. Assuming J_c to be the same for both samples, therefore, any change in trapped field can be attributed to a variation in k. The ratio of fields measured at the centre to the top of the two sample stack, $B_{(centre)}/B_{(top)}$, is 1.36 while predicted value (from equations (1) to (2)) is 1.56 (a difference of 15%). This deviation from the measured values is due to the fact that the Biot–Savart law assumes constant current density everywhere in the bulk sample whereas, in reality, central regions of the bulk are likely to have reduced J_c due to the relatively strong J_c-B dependence for MgB$_2$. It is also interesting to note that the magnitude of trapped field at the top of the stack (2.2 T) is similar to that observed at the top of a single bulk, suggesting that the increase in thickness of the MgB$_2$ sample contributes relatively little to the trapped field (i.e. the sample thickness of the single bulk has already reached the trapped field saturation limit). Significantly, no flux avalanches were observed to occur in the MPIG samples down to a minimum measurement temperature of 5 K, despite a relatively high trapped field.

The trapped field in the bulk MPIG samples fabricated in the current study is likely to be limited by moderate intrinsic values of J_c, at least compared to recently reported values of the order of MA/cm^2 in bulk MgB$_2$ fabricated by other processes [1, 35], and a strong *M–H* dependence. This also explains why only a 36% increase in the trapped field was observed at the centre of the two-sample stack compared to a single bulk.

Flux creep

The stability of trapped magnetic flux in the MgB$_2$ bulk samples was investigated further by performing additional magnetic moment measurements at 10 K following field
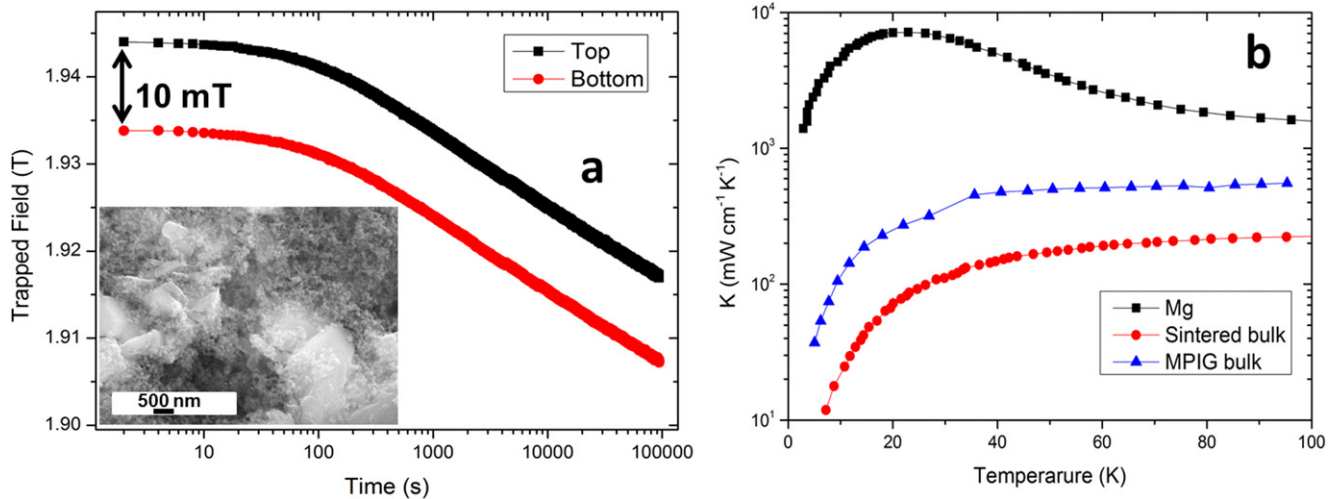
Figure 7. (a) Time dependence of magnetic field trapped in a bulk-MgB$_2$ sample fabricated by MPIG at 10 K and inset showing fine distribution of Mg and MgB$_2$ grains in inter-particle region. (b) Comparison of thermal conductivity of as processed MPIG [31], sintered MgB$_2$ (data from [37]) bulk and pure magnesium (data from [38]) as a function of temperature.

cooling at 5 T. Figure 7(a) shows variation of the trapped field with time for a single MgB$_2$ disc of diameter 32 mm. The trapped field after initial magnetization was measured to be 1.94 T, which decreased subsequently to 1.92 T (1% decay) and 1.91 T (1.5% decay), after 1 h and 1 d, respectively.

This behaviour is characteristic of logarithmic flux creep in type II superconductors (i.e. high initially and then decreasing rapidly to almost a linear variation after ~2 min) [36]. The flux creep behaviour of the sample measured in figure 7(a) can be expressed by the following equation;

$$B(T)/B(t(0)) = -0.004 \log(t) + 1 \quad \text{(For } t > 100 \text{ s)}. \tag{3}$$

The rate of loss of flux for these samples is relatively high compared to recent report by Yamamoto *et al* where the negative slope of B$(T)_{\text{(normalized)}}$ versus log(t) plot was as low as 4×10^{-6} [7].

During trapped field measurements, especially at low temperatures, dissipative flux motion can result in sudden local temperature rise. If this heat is not conducted away quickly enough, then it can potentially result in loss of trapped magnetic flux. Thus higher thermal conductivity is highly desirable in these quasi-permanent superconducting magnets [39].

Figure 7(b) describes measured thermal conductivity for MPIG bulk. Mg and sintered MgB$_2$ data are also plotted for a comparison. It is evident that thermal conductivity of MPIG bulk is significantly higher than a sintered bulk measured within 5–100 K. This is attributed to uniform distribution fine Mg grains in the inter-particle region (figure 7(a) (inset)) that possess orders of magnitude higher thermal conductivity than MgB$_2$. Detail SEM observation and EDS analysis suggests that such inter-particle regions (figure 7(a) inset) comprise of both MgB$_2$ and Mg grains.

As a result, it can be seen that thermal stability of samples has been increased and no flux avalanches were observed

down town to 5 K and magnetized bulk showed low trapped field decay rate.

Conclusion

Near-net shaped MgB$_2$ bulk superconductors have been fabricated by a MPIG method, incorporating MgB$_2$ powder in the precursor as wetting enhancer to facilitate in-flux of Mg, leading to a more uniform infiltration process. Almost identical value of trapped magnetic flux was measured at the top and bottom surfaces of a single bulk sample suggest that MgB$_2$ bulk samples fabricated by MPIG method are homogeneous. A stack of two MgB$_2$ bulk samples trapped a field of 3 T at the centre of the stack at 5 K. These values of trapped field are the highest obtained for single bulk MgB$_2$ sample or a combination of bulk samples fabricated by an infiltration growth process reported to date. Although, A moderate J_c and a strong J_c(B) dependence limits the overall trapped field performance of MgB$_2$ bulk superconductors fabricated by MPIG. The introduction of additional pinning centres to improve J_c in an applied magnetic field, therefore, is necessary for further improvement in trapped field performance of MgB$_2$ bulk fabricated by this technique. Finally, this study has demonstrated clearly that the IG method has significant potential for fabrication high quality, quasi-permanent MgB$_2$ magnets for high field applications.

Acknowledgments

References

[1] Fuchs G *et al* 2013 *Supercond. Sci. Technol.* **26** 122002

[2] Yamamoto *et al* 2015 *Int. Workshop on Processing and Applications of Superconducting (RE)BCO Large Grain Materials*

[3] Yamamoto A, Tanaka H, Shimoyama J, Ogino H, Kishio K and Matsushita T 2012 *Japan. J. Appl. Phys.* **51** 010105

[4] Giunchi G, Ripamonti G, Cavallin T and Bassani E 2006 *Cryogenics* **46** 237

[5] Giunchi G, Albsetti A F, Malpezzi L, Sagletti L and Perini E 2011 *Proc. 2011 IEEE Int. Conf. on Applied Superconductivity and Electromagnetic Devices 313*

[6] Sugino S, Yamamoto A, Shimoyama J and Kishio K 2015 *Supercond. Sci. Technol.* **28** 055016

[7] Yamamoto A, Ishihara A, Tomita M and Kishio K 2014 *Appl. Phys. Lett.* **105** 032601

[8] Naito T, Yoshida T and Fujishiro H 2015 *Supercond. Sci. Technol.* **28** 095009

[9] Durrell *et al* 2012 *Supercond. Sci. Technol.* **25** 112002

[10] Viznichenko *et al* 2003 *Appl. Phys. Lett.* **83** 4360

[11] Muralidhar M, Inoue K, Koblischka M R, Tomita M and Murakami M 2014 *J. Alloys Compd.* **608** 102

[12] Naito N, Sasaki T and Fujishiro H 2012 *Supercond. Sci. Technol.* **25** 095012

[13] Perini *et al* 2001 *IEEE Trans. Appl. Supercond.* **21** 2690

[14] Giunchi *et al* 2008 *IEEE Trans. Appl. Supercond.* **18** 1216

[15] Mochizuki H, Fujishiro H, Naito T, Albisetti A F and Giunchi G 2015 *Supercond. Sci. Technol.* **28** 105004

[16] Giunchi G 2003 *Int. J. Mod. Phys.* B **17** 453

[17] Canfield P C, Finnemore D K, Bud'ko S L, Ostenson J E, Lapertot G, Cunningham C E and Petrovic C 2001 *Phys. Rev. Lett.* **86** 2423

[18] Giunchi G, Ripamonti G, Raineri S, Botta D, Gerbaldo R and Quarantiello R 2004 *Supercond. Sci. Technol.* **17** S583

[19] Bhagurkar A G, Yamamoto A, Hari Babu N, Dennis A R, Durrell J H and Cardwell D A 2015 *Supercond. Sci. Technol.* **28** 015012

[20] Bhagurkar A G, Hari Babu N, Dennis A R, Durrell J H and Cardwell D A 2015 *IEEE Trans. Appl. Supercond.* **25** 6801504

[21] Dunand D C 2001 *Appl. Phys. Lett.* **79** 4186

[22] Ahn J H, Oh S, Wang X and Dou S X 2009 *Int. J. Mod. Phys.* B **23** 3503

[23] Naito T *et al* 2015 *Int. Workshop on Processing and Applications of Superconducting (RE)BCO Large Grain Materials* unpublished

[24] Iwayama I *et al* 2007 *Physica* C **460** 581

[25] Yamamoto A, Shimoyama J, Kishio K and Matsushita T 2007 *Supercond. Sci. Technol.* **20** 658

[26] Polyanskii A A *et al* 2007 *IEEE Trans. Appl. Supercond.* **17** 2746

[27] Aarstad K 2004 Protective films on molten Mg *PhD Thesis* Norwegian University of Science and Technology

[28] Chen D X and Goldfarb R B 1989 *J. Appl. Phys.* **66** 2489

[29] Klie R F, Idrobo J C, Browning N D, Regan K A, Rogado N S and Cava R J 2001 *Appl. Phys. Lett.* **79** 1837

[30] Fujishiro H, Naito T and Yoshida T 2014 *Supercond. Sci. Technol.* **27** 065019

[31] Zou J *et al* 2015 *Supercond. Sci. Technol.* **28** 075009

[32] Yamamoto A *et al* 2011 MgB_2 bulk superconducting magnet *Abstracts of the 15th Japan–US Workshop on Advanced Superconductors* (arXiv:1208.185)

[33] Sasaki T, Naito T and Fujishiro H 2013 *Phys. Procedia* **45** 93

[34] Johansen T 2000 *Supercond. Sci. Technol.* **13** R121

[35] Prikhna T A *et al* 2014 *Supercond. Sci. Technol.* **27** 044013

[36] Beasley M R, Labusch R and Webb W W 1969 *Phys. Rev.* **181** 682

[37] Bauer E *et al* 2001 *J. Phys.: Condens. Matter* **13** L487

[38] Ying T, Chi H, Zheng M, Li Z and Uher C 2014 *Acta Mater.* **80** 288

[39] Tomita M and Murakami M 2003 *Nature* **421** 517